JOURNAL OF CATALYSIS 96, 154–169 (1985)

The Redispersion of Iridium on SiO_2 and γ-Al_2O_3 Supports with Chlorine-Containing Gases

K. FOGER, D. HAY, AND H. JAEGER

CSIRO Division of Materials Science, Locked Bag 33, Clayton 3168 Australia

Received January 16, 1985; revised May 12, 1985

Iridium metal particles (1–100 nm in size) on SiO_2 (Aerosil, Degussa) and γ-Al_2O_3 (Merck, 125 m^2 g^{-1}) supports have been exposed in a flow system at selected temperatures in the range 470–830 K to Cl_2 or HCl mixed with one or two of the following gases: N_2, He, O_2, H_2O, NO, CO or air. The extent of reaction and its effectiveness for the redispersion of agglomerated iridium metal was examined with X-ray diffraction (XRD), transmission electron microscopy (TEM), UV-diffuse reflectance spectroscopy, and temperature-programmed reduction (TPR). α-$IrCl_3$ was formed exclusively on SiO_2 and Al_2O_3 by treatment with Cl_2. At $T_r < 750$ K it built up in layers around Ir particles, but at higher T_r enhanced mobility resulted in the formation of thin $IrCl_3$ sheets. Transport could be induced at lower temperatures, by the addition of O_2, H_2O, CO, or NO to the treatment stream. However, under most conditions crystalline products ($IrCl_3$, IrO_2, $Ir(CO)_3Cl$) were formed which converted on reduction into large Ir agglomerates. A dispersed product phase which yielded small Ir particles on reduction was present on γ-Al_2O_3 after treatment with Cl_2 + CO ($4 < Cl_2/CO < 2.5$) or with Cl_2 + NO ($Cl_2/NO > 2$) in N_2. The products are believed to be anionic iridium carbonyl- or nitrosyl-chloride complexes anchored on the alumina surface.

INTRODUCTION

Reforming catalysts consist of very small platinum-group metal particles on a refractory oxide support. In use catalysts gradually lose activity as a result of carbon deposition and agglomeration of metal particles. During regeneration catalysts are exposed sequentially at elevated temperatures to atmospheres containing as principal reacting agents (i) oxygen to "burn-off" the carbon, (ii) halogen to redisperse the metal as halide, and (iii) hydrogen to reduce the halide to the metal. Typical regeneration sequences are described in numerous publications (*1, 2*). More recently, redispersion procedures especially suited for catalysts which contain iridium have been reported (*13*).

Oxygen treatment at temperatures above 500 K proved extremely detrimental to iridium catalysts in particular, since the formed highly volatile IrO_2 agglomerates to large crystals (*3*).

Recently, we have studied the redispersion of agglomerated platinum on SiO_2 and γ-Al_2O_3 supports with Cl_2 over a wide range of conditions using transmission electron microscopy (TEM), UV-diffuse reflectance spectroscopy, X-ray diffraction (XRD), and temperature-programmed reduction (TPR) to examine the catalysts at various stages of treatment (*4*). Here we have used the same methods to determine whether iridium metal particles on SiO_2 or γ-Al_2O_3 can be dispersed by treatment with Cl_2 or HCl mixed with one or two of the following gases: N_2, He, O_2, H_2O, NO, CO, and air.

EXPERIMENTAL

Experiments were carried out with a wide range of size distributions of Ir particles on various SiO_2 and Al_2O_3 supports, but the results are reported for three model catalysts.

Catalysts 1 (1.8 wt% Ir on SiO_2). Aerosil 200 (Degussa) was impregnated to incipient dryness with $(NH_4)_2IrCl_6$ in H_2O, dried in air at 400 K, and reduced in flowing H_2 at 670 K for 15 hr. The Ir particles (Fig. 1a)

0021-9517/85 $3.00

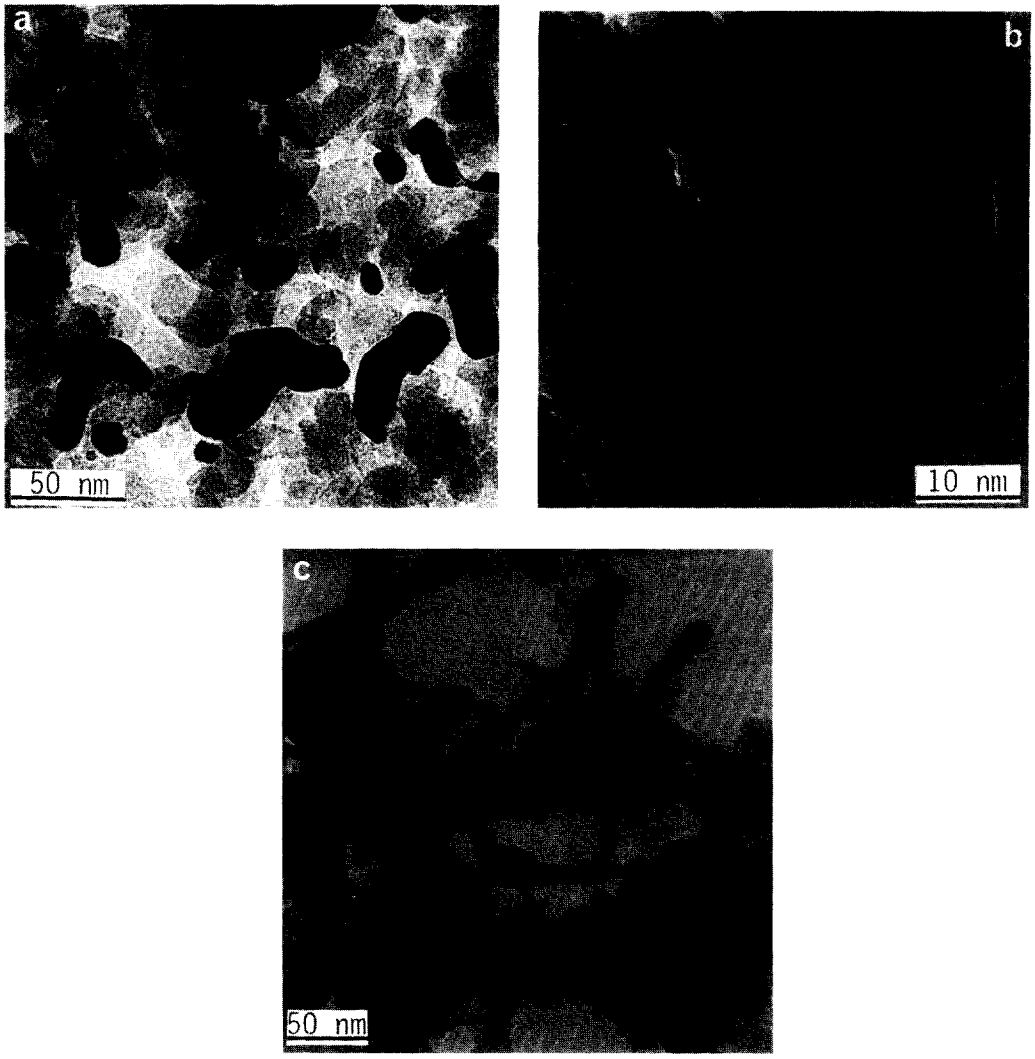

FIG. 1. Electron micrographs of (a) catalyst 1, (b) catalyst 2, and (c) catalyst 3.

varied from 3 to 20 nm, with a mean, $\bar{d}_{Ir}$, of 10 nm.

Catalyst 2 (2.3 wt% Ir on γ-Al_2O_3). $Ir_4(CO)_{12}$ was deposited onto γ-Al_2O_3 (Merck, 125 $m^2\ g^{-1}$) from cyclohexane. The solvent was evaporated and the carbonyl decomposed in flowing N_2 at 620 K, and reduced in H_2 at 670 K. The Ir particles had diameters, d_{Ir}, of about 1 nm (Fig. 1b).

Catalyst 3 (3.0 wt% Ir on γ-Al_2O_3). The support (Merck, 125 $m^2\ g^{-1}$) was impregnated with $(NH_4)IrCl_6$ in H_2O, dried in air at 400 K, and exposed to flowing H_2 at 670 K for 15 hr, and then to 1 vol% O_2/He at 820 K for 2 hr. This was followed by retreatment in flowing H_2 at 670 K for 15 hr. Most of the Ir was in the form of clusters of polycrystalline needles (up to 200 nm long), shown in Fig. 1c.

Catalyst samples (0.5–1.0 g) were placed in an externally heated vertical fused-silica reactor tube and exposed at atmospheric pressure for predetermined durations, t_r ($0.5 < t_r < 15$ hr), and selected temperatures, T_r, ($470 < T_r < 830$ K) to flowing Cl_2 in N_2, $Cl_2 + O_2$ in He, $Cl_2 + H_2O$ in air, $Cl_2 + CO$ in N_2, $Cl_2 + NO$ in N_2, or $HCl + O_2$ in He (total flow rate, 1.8 liters hr^{-1}). The

exposure was terminated by flushing with N_2 or He and cooling to room temperature. The catalyst samples were then removed and examined as previously described (*4*). Products were identified from peak positions in XRD traces (Fig. 2), from imaging of lattice planes and selected-area diffraction in the TEM, and by comparing UV-diffuse reflectance spectra of the samples with those of otherwise identified compounds mixed intimately with the support. When $IrCl_3$ was the exclusive product, the extent of conversion of Ir was determined from the H_2 consumption during TPR assuming a stoichiometry of 1. 5 moles H_2 per mole $IrCl_3$. A comparison of the areas under the Ir 111 peaks in XRD traces before and after exposure gave results in agreement with the TPR data in the case of catalyst 1.

RESULTS

Values for the conversion of Ir particles in the three catalysts after reactions in the treatment mixtures at selected temperatures and times are given in Table 1, which also lists the products.

Exposure to Cl_2

When any one of the catalysts was exposed to Cl_2, either pure or mixed with N_2, products were observed to accumulate on the outside of Ir particles after about 3 hr exposure at T_r = 650 K (Fig. 3a). Increasing T_r caused a more rapid buildup of reaction products encapsulating the Ir (Figs. 3b–d). Thus separate Ir particles gave rise to product particles several times larger, but of the shapes of the originating Ir particles. The product envelopes of particles in close proximity often merged during prolonged reaction to provide an outline of the original assembly of metal particles (Fig. 3b). Generally no gaps could be seen between the outer surface of the residual Ir particles and the inner surface of the product envelopes. However, when Ir particles were completely converted to the chloride, hollow

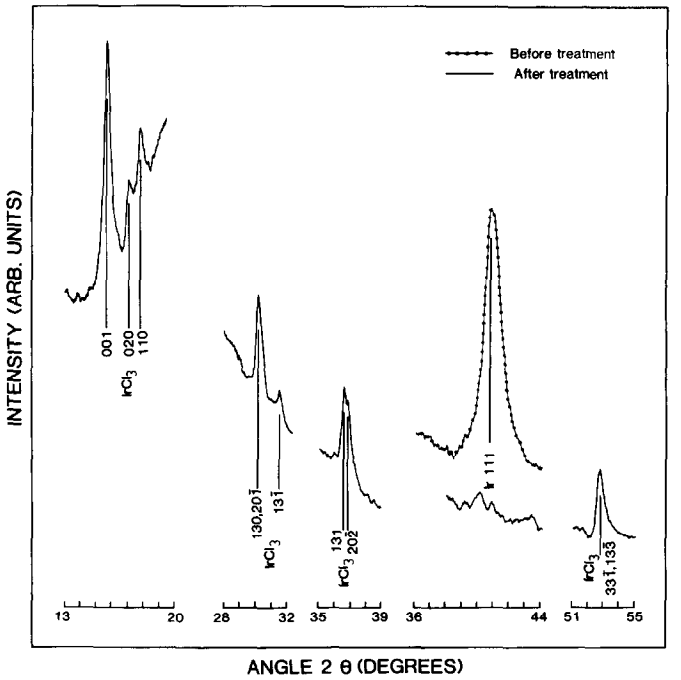

FIG. 2. XRD scan of catalyst 1 before and after treatment in 10 vol% Cl_2 in N_2 at T_r = 700 K and t_r = 3 hr. Radiation: Cu$K\alpha$ (Ni filtered).

TABLE 1

Results of the Reaction of Chlorine with the Catalysts

Catalyst	Treatment			% Metal converted	Product
	Gas composition (vol%)	Temp., T_r (K)	Time, t_r (hr)		
1) 1.8% Ir/SiO_2	10% Cl_2	683	1.5	40	$IrCl_3$[a]
	90% N_2		3.0	50	
			15.0	65	
		700	3.0	65	
		740	1.0	65	
		830	0.6	100	
	10% Cl_2	690	3.0	50	$IrCl_3$[a]
	1% O_2	755	1.5	90	$IrCl_3$ IrO_2[a]
	89% He	810	0.6	100	IrO_2
	10% Cl_2	750	1.0	60	$IrCl_3$[a]
	2% H_2O	780	1.0	95	
	88% air				
	10% HCl	770	2.0	60	$IrCl_3$[a]
	1% O_2				
	89% He				
2) 2.3% Ir/Al_2O_3	10% Cl_2	670	2.0	65	$IrCl_3$[b]
	90% N_2	720	0.5	100	
3) 3% Ir/Al_2O_3	10% Cl_2	680	3.0	20	$IrCl_3$[a]
	90% N_2	710	5.0	52	
		810	2.0	85	
	6.7% Cl_2	670	1.0	55	Dispersed phase,[c,d] some $IrCl_3$[a]
	1.3% NO		3.0	100[c]	
	90% N_2				
	5% Cl_2	670	1.0	100	Mainly $IrCl_3$,[a] some dispersed phase[d]
	5% NO				
	90% N_2				
	8.5% Cl_2	620	2.0	30	Mainly $IrCl_3$,[a] some dispersed phase[d]
	1.5% CO				
	90% N_2				
	8% Cl_2	570	3.0	50	Dispersed phase[d]
	2% CO				
	90% N_2				
	5% Cl_2	570	1.0	100	$Ir(CO)_3Cl$[a]
	5% CO				
	90% N_2				

[a] Crystalline phase (identified by XRD and TEM).
[b] Identified by UV–Vis diffuse reflectance spectroscopy.
[c] Phase predominates.
[d] Unidentified.

envelopes were sometimes observed; for example, a comparison of Figs. 3e and f shows the 0.57-nm interlayer spacing only in the outer shells of the particle but not in the center. Complete conversion of very small Ir particles (catalyst 2, $\bar{d}_{Ir} < 1$ nm) to products required $t_r = 0.5$ hr at $T_r = 720$ K (compare Figs. 4a and b), while for catalyst 1,

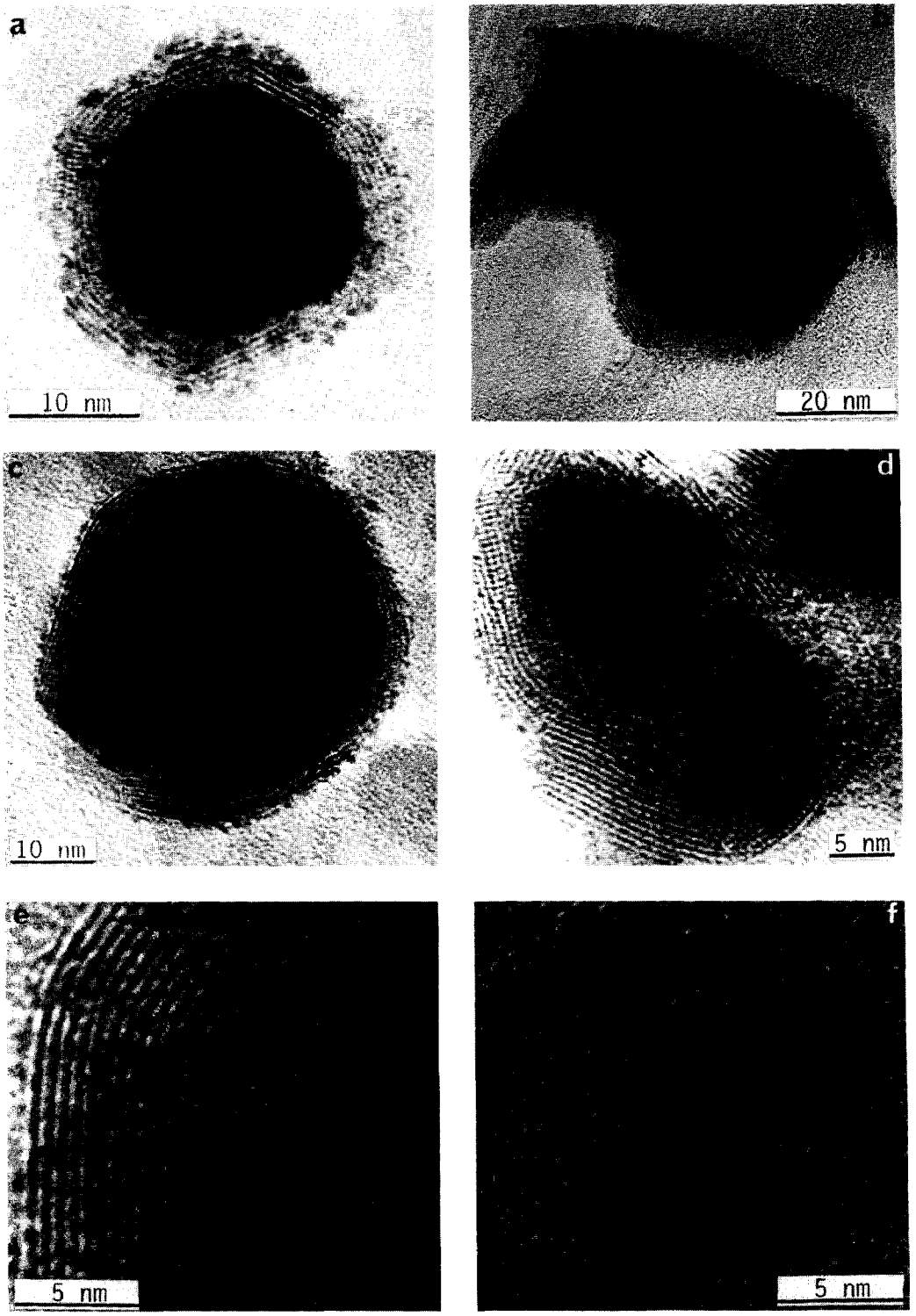

FIG. 3. TEM images of iridium chlorides formed in 10 vol% Cl_2 in N_2 on SiO_2 (catalyst 1): (a) $T_r = 680$ K, $t_r = 3$ hr; (b) $T_r = 700$ K, $t_r = 3$ hr; (c) $T_r = 830$ K, $t_r = 0.6$ hr; and on Al_2O_3 (catalyst 3): (d) $T_r = 810$ K, $t_r = 2$ hr. Part of the image of the chloride particle shown in (c) at higher magnification: (e) edge and (f) center. The spotty appearance of $IrCl_3$ in these and the following figures results from decomposition in the electron beam.

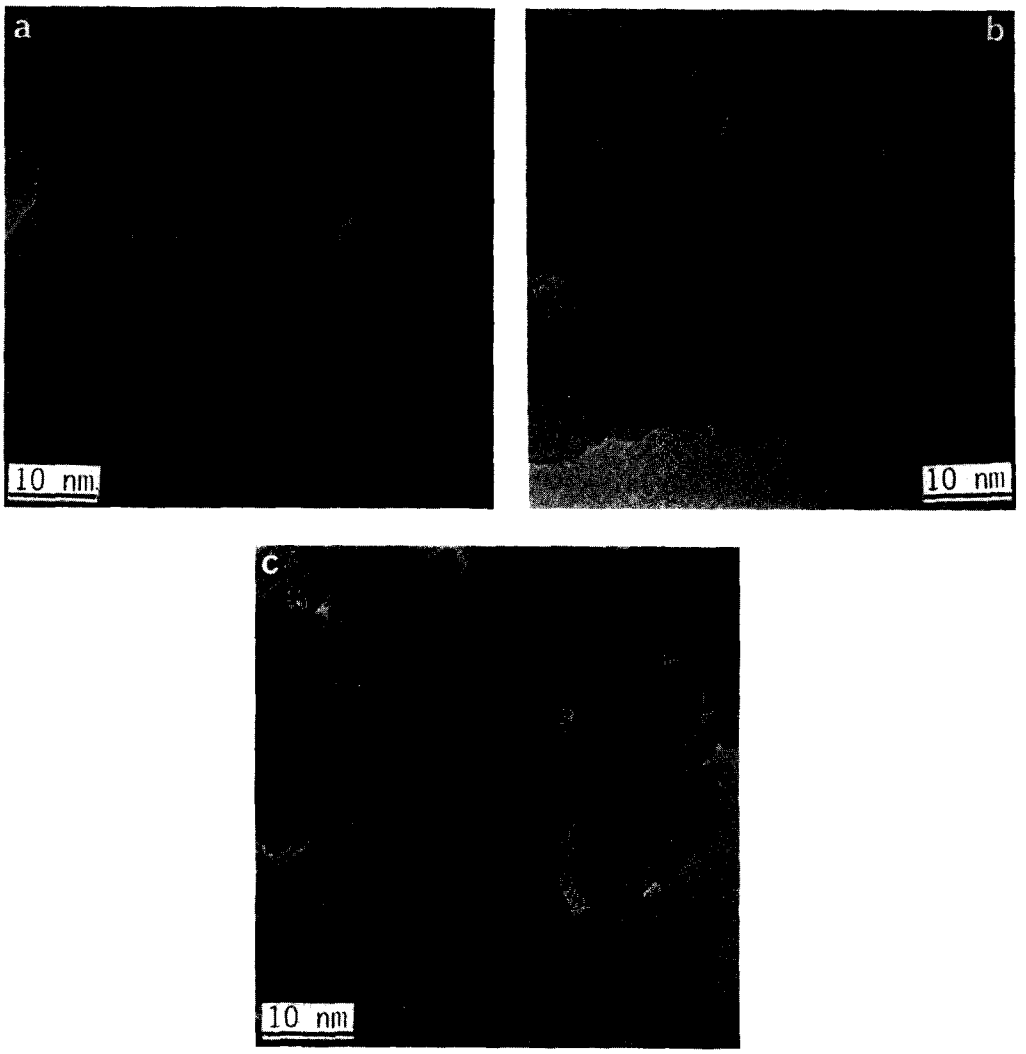

FIG. 4. Electron micrographs showing the effects of treatment in 10 vol% Cl_2 in N_2 at T_r = 720 K and t_r = 0.5 hr on the size and spatial distribution of Ir particles in catalyst 2: before treatment (a), after treatment followed by reduction (c). The formed chloride was not visible by TEM (b).

$\bar{d}_{Ir}$ = 10 nm, a reaction temperature, T_r, of 830 K was necessary for complete conversion in the same reaction time.

Inspection of large numbers of TEM images showed the product always to be crystalline with an interlayer spacing as reported for α-$IrCl_3$, viz, 0.57 nm (*5*). Because the product formed envelopes, other spacings reported for α-$IrCl_3$ could not be verified with either imaging or selected-area diffraction in the TEM. When the original metal particles were large (catalysts 1 and 3), examination of XRD traces (e.g., Fig. 2) confirmed that the reaction produced exclusively α-$IrCl_3$. For catalyst 2, $\bar{d}_{Ir}$ = 1 nm, no products were observed with TEM or XRD, but UV-diffuse reflectance spectra were identical to those obtained from a mixture of α-$IrCl_3$ and alumina.

No appreciable transport of reaction products occurred during exposure to Cl_2 at T_r < 750 K; only layer buildup around Ir particles was observed. Further evidence for the lack of mobility of the chloride is illustrated in Figs. 4a and c, which show

that the spatial and size distributions of Ir particles did not change when catalyst 2 was exposed to 10% Cl_2 in N_2, t_r = 0.5 hr, T_r = 720 K, and subsequently subjected to TPR. However, for $T_r > 750$ K, the occasional appearance of thin sheets of α-$IrCl_3$ in addition to envelopes indicated the onset of some product transport.

Exposure to Cl_2 + O_2

The presence of small amounts of O_2 with the Cl_2 in the treatment gas did not significantly influence the reaction at $T_r < 700$ K, but above this temperature the morphology of the products changed (see Table 1). At T_r = 770 K, two distinct products could be identified in TEM images (e.g., Figs. 5d and f). One appeared to be α-$IrCl_3$ and formed layers of 0.57 nm following the surface contours of the Ir particles. The other exhibited a lattice spacing consistent with that for IrO_2, viz, 0.32 nm (*6*). For T_r = 810 K, only IrO_2 was observed as large, separate single-crystal sheets (Figs. 5c and e). The transport of reaction products observed with Cl_2 + O_2 as the reactant was slightly higher than that with just Cl_2, but lower than that seen previously with O_2 alone (*3*). As T_r was progressively raised above 770 K, products were increasingly lost from both SiO_2 and γ-Al_2O_3 supports. We have been unable to identify the transported species. Material condensed in colder parts of the reactor outlet consisted of at least two compounds. Some dissolved in water to give a deep-blue solution, similar to that from $IrCl_3 \cdot H_2O$. XRD traces of condensate collected on SiO_2 revealed weak reflections in positions close to but not identical with those resulting from IrO_2. From a comparison of the present observations with those made previously on the reaction of O_2 alone with Ir particles on SiO_2 (*3*), we suggest that the transported species is an oxychloride of Ir.

Exposure of Cl_2 + H_2O in Air and HCl + O_2 in He

Cl_2 in wet air produced exclusively $IrCl_3$ (Figs. 5b and d). This was also the case when the catalysts were exposed to HCl and O_2, but no reaction was observed with HCl alone. With both combinations of reactants, the product showed a marked tendency to form separate sheets of $IrCl_3$ in addition to envelopes around Ir particles, indicating enhanced transport (Fig. 6).

Exposure to Cl_2 + CO

When catalysts were exposed to mixtures of Cl_2 and CO the rate of attack on the Ir particles was markedly increased compared to that observed for similar concentrations of Cl_2 alone. For example, examination of Table 1 shows that treatment of catalyst 3 in 10% Cl_2 in N_2 at 680 K resulted in 20% conversion after 3 hr, but exposure to 8.5% Cl_2 + 1.5% CO in N_2 resulted in 30% conversion after only 2 hr at 620 K. The main product observed with XRD or TEM up to this relative concentration of CO (Cl_2/CO > 4) was $IrCl_3$. As illustrated in Fig. 7a, residual metal particles were enveloped in thick layers, the structure and morphology of which in no way differed from those observed on exposure to Cl_2 alone.

In the range (4 > Cl_2/CO > 2.5) another marked increase in the rate of attack on Ir particles was observed. On γ-Al_2O_3 the reaction produced a highly dispersed product phase which could not be detected by TEM or XRD, but was deduced from the observation that small Ir particles ($\bar{d}_{Ir} < 4$ nm) were seen on electron micrographs after subsequent reduction (Fig. 11e). On SiO_2 the reaction produced large crystals of $IrCl_3$.

Exposure to Cl_2 and CO in ratios < 2 resulted in appreciable attack on Ir at $T_r >$ 470 K. The product formed needle-shaped crystals which varied widely in size. Small needles usually appeared to be solid, but large ones were apparently hollow (Fig. 7c). Isolated needles were occasionally observed on the substrate, but more often needles formed "pincushion" structures (Fig. 7b). Selected area diffraction of large

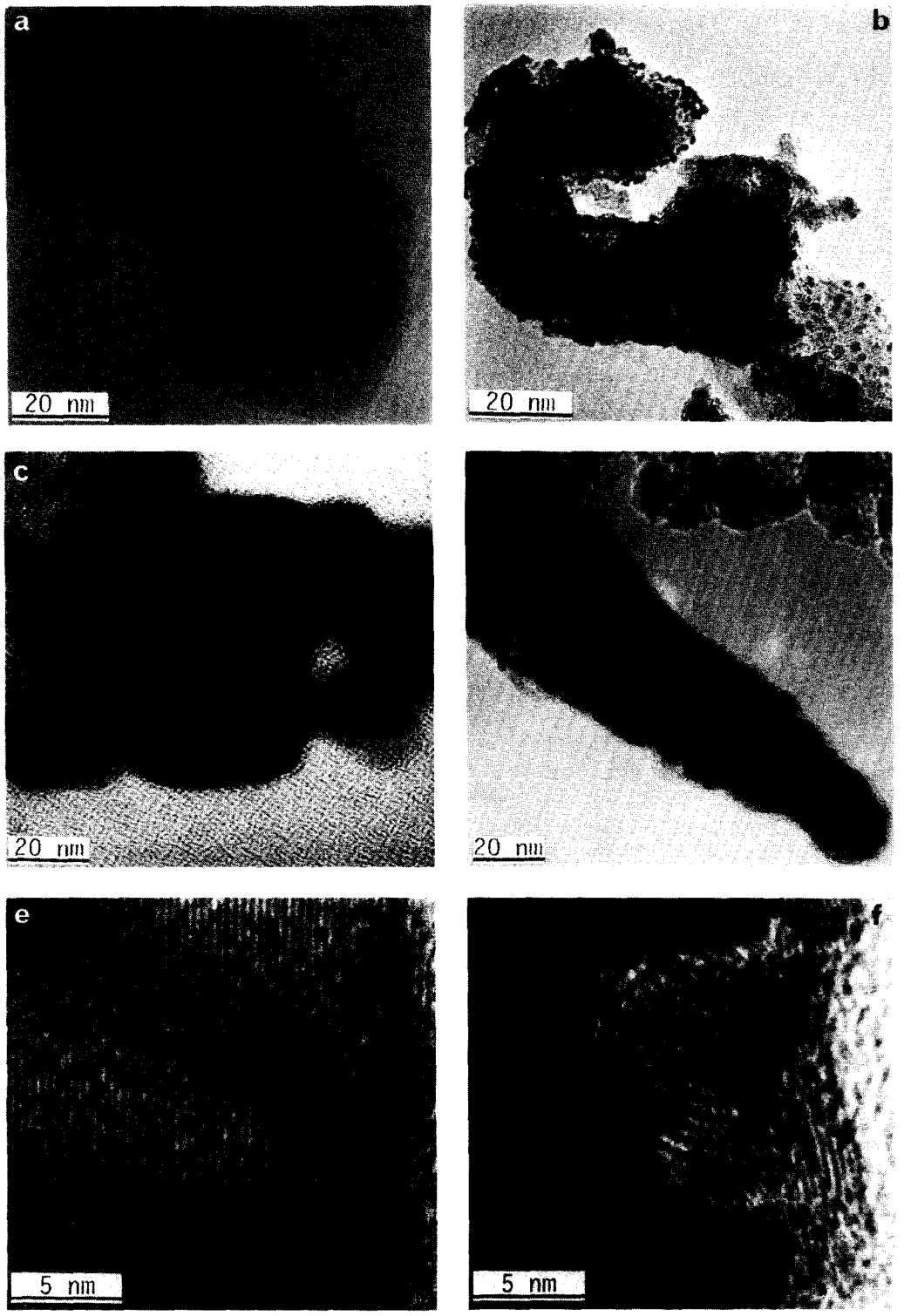

FIG. 5. TEM images of catalysts treated with: (a) 10 vol% Cl_2 and 2 vol% H_2O in air, catalyst 1, T_r = 780 K; (b) catalyst 3, T_r = 720 K, and (c) with 10 vol% Cl_2 in 1 vol% O_2 in He, catalyst 1, T_r = 810 K; (d) catalyst 3, T_r = 770 K. Lattice images of particles in (c) and (d) are shown in (e) and (f). Only IrO_2 spacings are visible in (e); both IrO_2 and $IrCl_3$ spacings are present in (f).

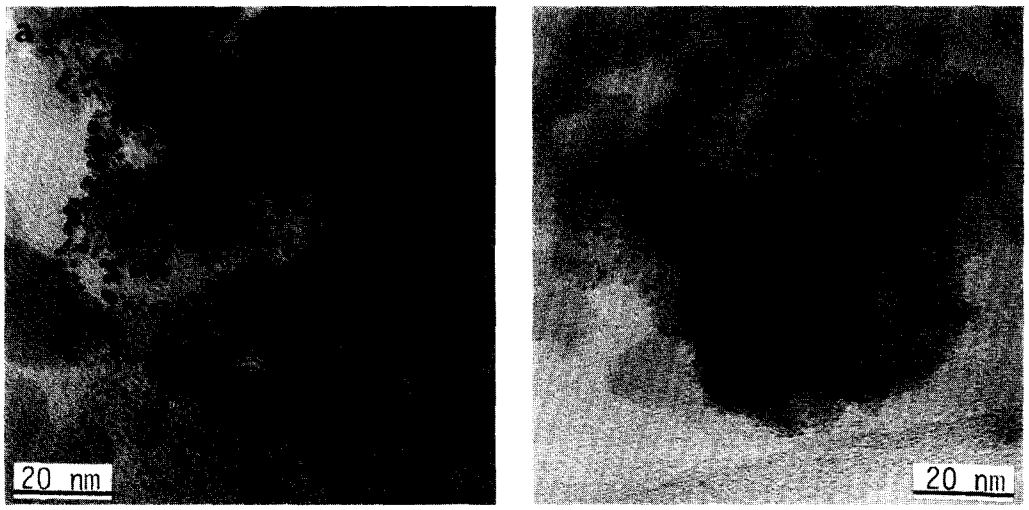

FIG. 6. Electron micrographs showing morphologies of iridium chloride on SiO_2 formed by treatment of catalyst 1 in 10 vol% HCl in 1 vol% O_2 in He at T_r = 770 K and t_r = 2 hr.

needles showed sets of regularly spaced spotty streaks normal to the needle axis, indicating that the needles were single crystals with faults parallel to the long axis. However, it is not possible to say whether the faults are tubular or linear. On prolonged exposure, Ir was lost from the support at T_r as low as 570 K. When the transported products were condensed on SiO_2 in cold parts of the reactor outlet, XRD traces showed distinct peaks which did not match any published powder-diffraction pattern for Ir compounds. From the crystal habit and the color of the treated samples, we conclude that the transported material is most likely $Ir(CO)_3Cl$ (7).

Exposure to Cl_2 + NO

Adding NO to Cl_2 also increased the rate of attack on Ir, but to a lesser extent than CO. For example, all the Ir in catalyst 3 was converted with 5% Cl_2 + 5% CO in N_2, T_r = 570 K in 1 hr, but with 5% Cl_2 + 5% NO in N_2 as the reacting gas, T_r = 670 K was required for the same converison (cf. Table 1).

After treatment of catalyst 3 in gas mixtures in the range $Cl_2/NO > 2$, the outlines of residual Ir particles were no longer smooth (Fig. 8a). After short reaction times irregular thin sheets, often in the vicinity of residual Ir particles, were observed (Fig. 8b). These sheets, which readily decomposed into contiguous networks of very small Ir particles during visual examination in the TEM, where shown by selected-area diffraction to be single crystals of $IrCl_3$. On γ-Al_2O_3 substrates the presence of an additional highly dispersed phase was deduced from the observation that small metal particles were apparent after reduction. This phase predominated at high Cl_2 to NO ratios and longer reaction times, but its proportion decreased with increasing NO concentration in the treatment gas. When the treatment gas contained Cl_2 and NO in ratios ≤ 1, thicker, regularly shaped sheets of $IrCl_3$ were formed (Fig. 8d) which also decomposed in the electron beam (Fig. 8c). On SiO_2 substrates a highly dispersed produce phase was never found, either before or after reduction.

Temperature-Programmed Reduction

TPR profiles strongly depend on the degree of conversion of iridium metal in the catalysts to chloride compounds.

(1) Figure 9, which presents TPR traces of iridium on SiO_2, shows peaks for selected values of conversions as follows: (i)

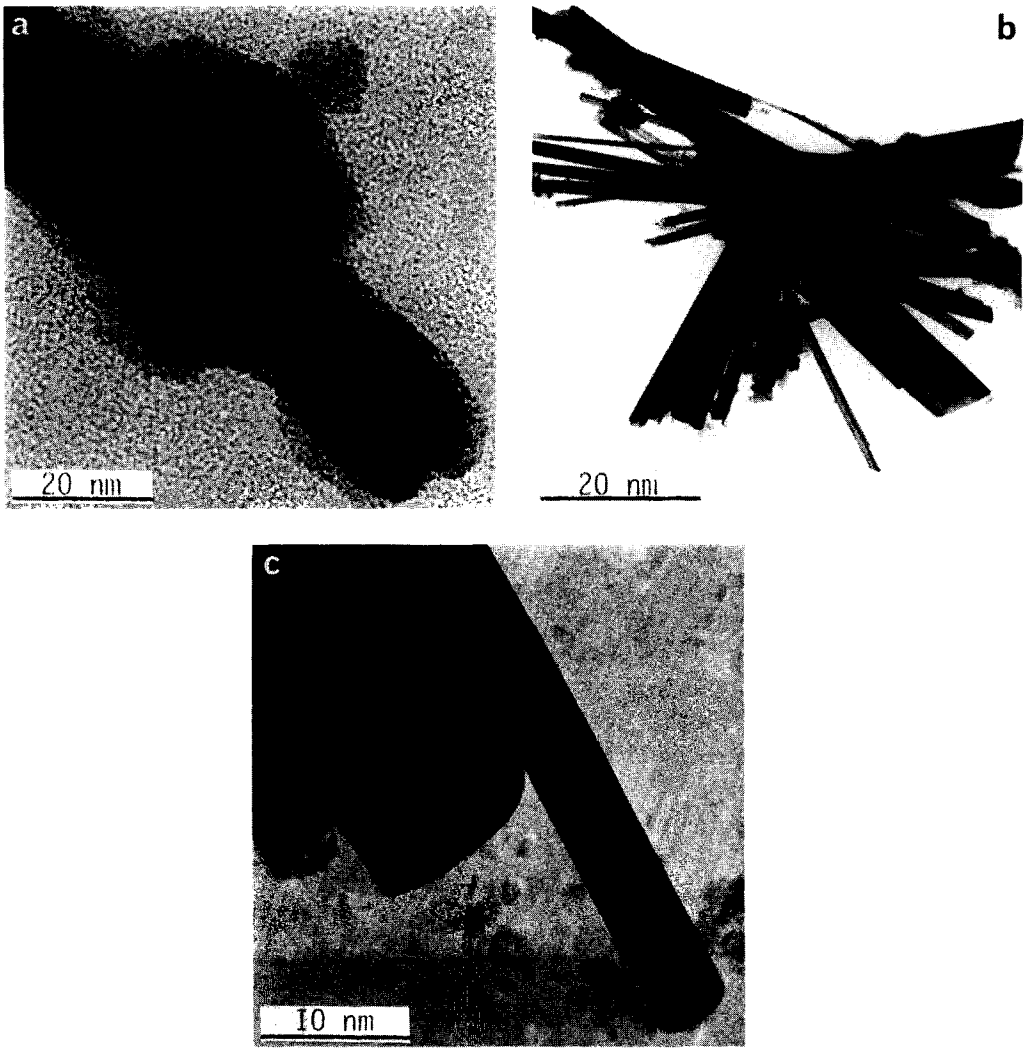

FIG. 7. Electron micrographs of catalyst 3 treated with 10 vol% Cl_2–CO in N_2: (a) $CO/Cl_2 = 0.17$, $T_r = 620$ K, $t_r = 2$ hr; (b) $CO/Cl_2 = 1$, $T_r = 570$ K, $t_r = 1$ hr; and (c) $CO/Cl_2 = 1$, $T_r = 470$ K, $t_r = 2.5$ hr.

a single sharp peak at 440 K for 40% conversion and at 510 K for 100% conversion, (ii) a broad peak at about 470 K for 65% conversion, (iii) a sharp peak at 440 K with a broad shoulder at 500 K for 50% conversion, and (iv) a peak around 500 K with a narrow shoulder at around 450 K for 90% conversion.

(2) Figure 10 shows TPR traces of chlorine-treated Ir on γ-Al_2O_3. For catalyst 3 (large needle-shaped Ir particles), two broad peaks at 410 and 500 K are seen when the conversion is low (about 20%), and when 85% of the Ir is converted, a peak at 500 K with a slight shoulder at 430 K is observed. For catalyst 2, with only very small Ir particles, TPR traces for 65 and 100% conversions show only single peaks at 470 K.

Morphology of Ir after Exposure and Reduction

The reduction of $IrCl_3$ envelopes produced agglomerates of Ir crystallites which often preserved the outline of the originating chloride crystals (Fig. 11a). These ag-

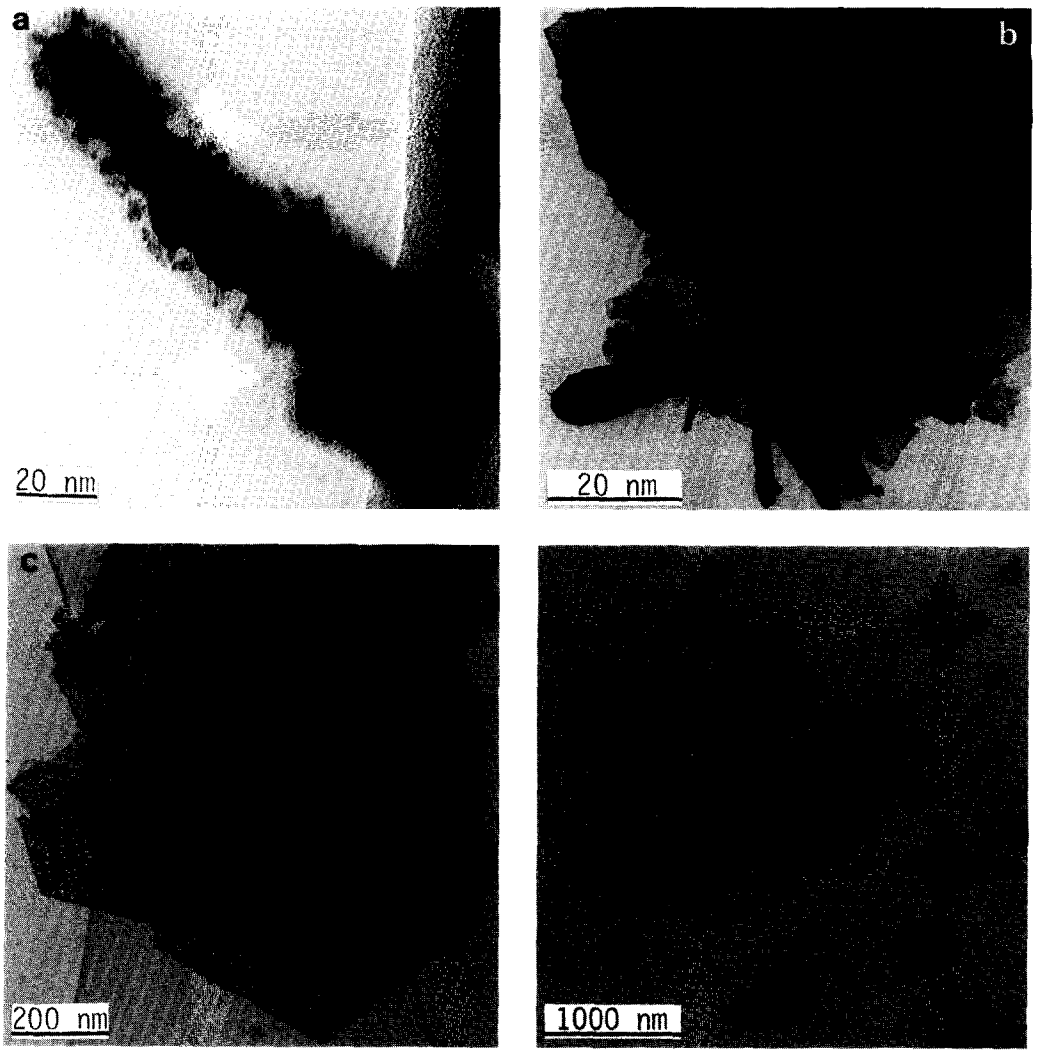

FIG. 8. Electron micrographs of catalyst 3 treated at (a, b) T_r = 670 K and t_r = 1 hr in 6.7 vol% Cl_2 and 3.3 vol% NO in N_2, and (c, d) in 5 vol% Cl_2 and 5 vol% NO in N_2.

glomerates sintered readily at elevated temperatures to yield metal particles, similar to or even larger than those originally present in the catalysts. Evidence from XRD showed that the treatment sequence produced no significant change in crystallite size.

Thin $IrCl_3$ sheets, which were observed after exposure to gas mixtures containing as reactants $Cl_2 + O_2 + H_2O$, $Cl_2 + NO$, and $HCl + O_2$, changed on reduction to contiguous aggregates of small crystallites (Figs. 11b,c). The aggregates also sintered readily to produce assemblies of large Ir crystallites evidenced by sharp XRD peaks. The crystalline needles, which we believe are iridium carbonylchloride, transformed on reduction into acicular Ir agglomerates (Fig. 11d).

The highly dispersed product phase, which formed only on γ-Al_2O_3 substrates (catalyst 3), produced small, evenly distributed Ir particles on reduction (Figs. 11e and f).

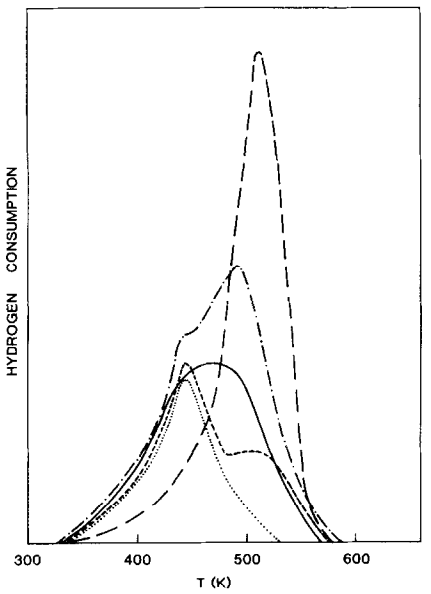

FIG. 9. Temperature-programmed reduction profiles for catalyst 1 treated in 10 vol% Cl_2 in N_2: T_r = 680 K, t_r = 1.5 hr (...); T_r = 680 K, t_r = 3 hr (– – –); T_r = 740 K, t_r = 1 hr (———); T_r = 760 K, t_r = 1.5 hr (·–·–·); T_r = 820 K. t_r = 0.6 hr (— —). Weight of sample, 0.1 g; temperature increase, 10 K min^{-1}.

DISCUSSION

Reaction of Iridium

(*i*) *With Cl_2.* Direct chlorination of Ir metal results exclusively in the formation of monoclinic α-$IrCl_3$ (*5*), which, on prolonged heating at 1020 K transforms into orthorhombic β-$IrCl_3$ (*8*). In agreement with this we also observed exclusively α-$IrCl_3$ mostly as envelopes around metal particles, but sometimes as separate thin sheets. The product layer buildup inhibits the overall reaction. Examination of Table 1 shows that for catalyst 1 ($\bar{d}_{Ir}$ = 10 nm), reaction with 10% Cl_2 in N_2 at T_r = 670 K resulted in 40% conversion of Ir after t_r = 1.5 hr, 50% after t_r = 3.0 hr, and 65% after t_r = 15 hr. The same trend is confirmed by the observation that the 1-nm particles of catalyst 2 were completely converted in the same mixture at T_r = 720 K after 0.5 hr, whereas in catalyst 3, which contained large Ir needles, only 50% of the metal was converted after 5 hr. The strong deceleration of the reaction with time together with the observations that (i) the resulting chloride envelopes are coherent up to a thickness of at least 10 nm at T_r < 750 K, (ii) no gaps are present between the product and the residual metal, and (iii) product envelopes are several times larger than the original metal particles, suggest a diffusion-controlled topochemical reaction. The scheme involves, after the fast buildup of the initial product layer, diffusion of the reactant through this layer to the interface with the metal, then reaction at the interface and diffusion of the formed ions to the outside of the envelopes. At T_r above 750 K, iridium chloride becomes volatile as indicated by the increased tendency to form separate thin sheets, and total conversions of Ir to $IrCl_3$ are achieved more rapidly.

(*ii*) *With Cl_2 + CO and Cl_2 + NO.* Addition of CO or NO to the reaction stream markedly accelerates the chlorination of iridium. The accelerating effect of CO has been known for many years and is, for example, used in the preparation of $IrCl_3$ from

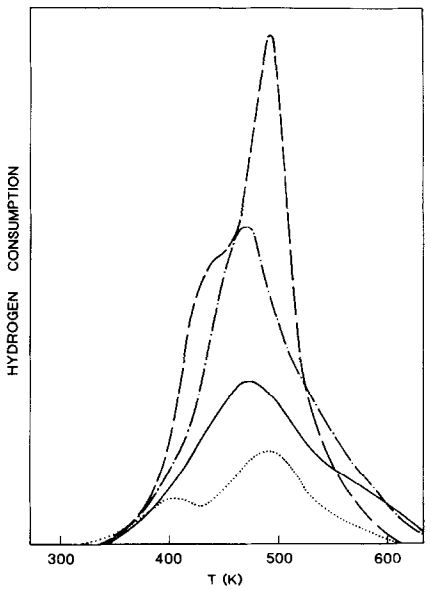

FIG. 10. Temperature-programmed reduction traces for catalysts 2 and 3 treated in 10 vol% Cl_2 in N_2. Catalyst 2: T_r = 670 K, t_r = 2 hr (———); T_r = 720 K, t_r = 0.5 hr (–·–·). Catalyst 3: T_r = 680 K, t_r = 3 hr (...); T_r = 810 K, t_r = 2 hr (– – –). Weight of sample, 0.1 g; temperature increase, 10 K min^{-1}.

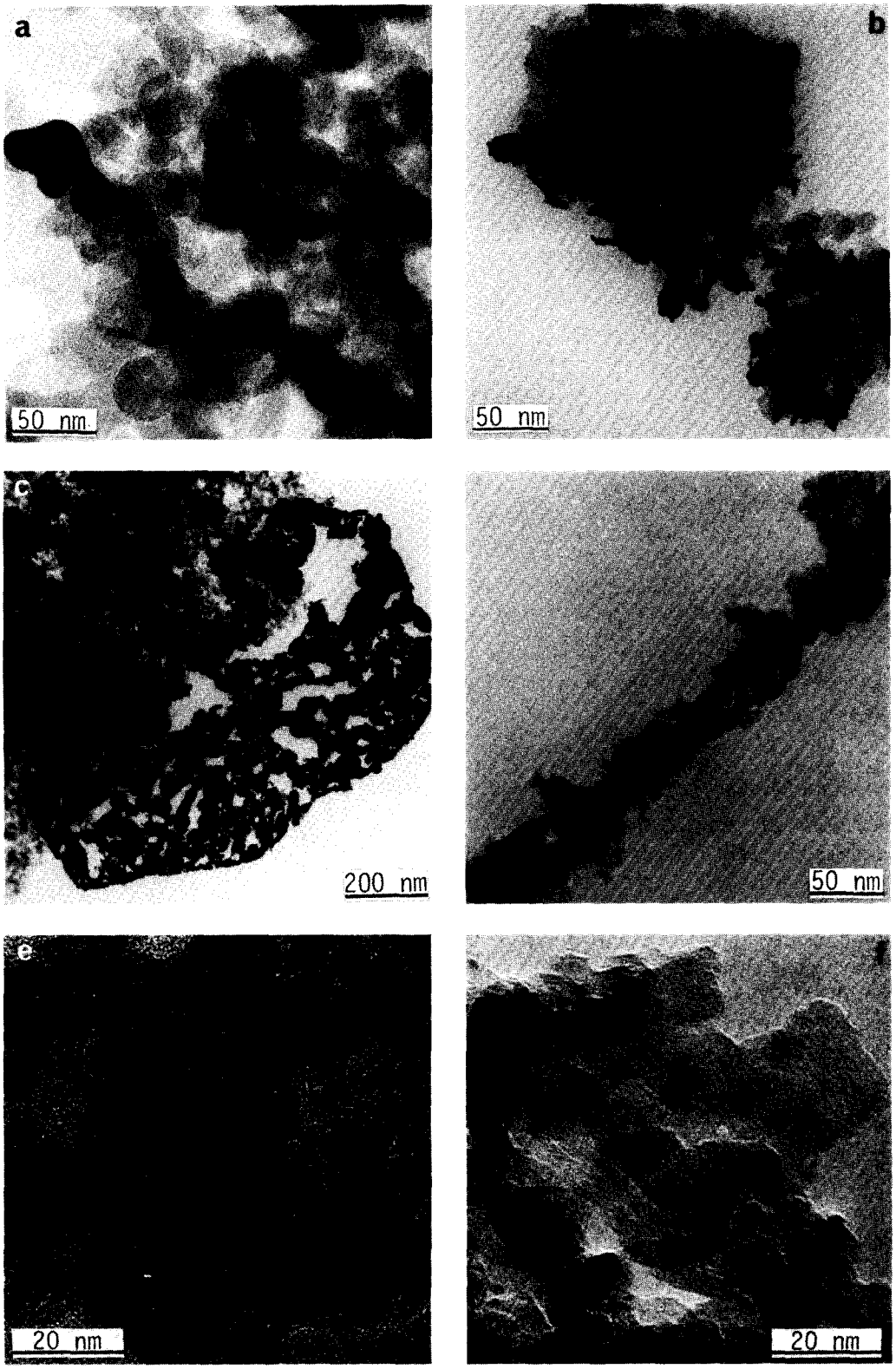

FIG. 11. TEM images of Ir particles obtained by reduction of (a) $IrCl_3$ envelopes on SiO_2; (b, c) $IrCl_3$ sheets on SiO_2; and (d) $Ir(CO)_3Cl$ needle on Al_2O_3. (e, f) The highly dispersed product phases obtained in Cl_2/CO (ratio 4/2.5) and in Cl_2/NO (ratio > 2) transform on reduction into small Ir particles.

Ir powders (*9*). The action of CO has been attributed to the formation and decomposition of $COCl_2$, yielding highly active chlorine atoms. Furthermore, the accelerating effect of both CO and NO in the reaction of Ir with Cl_2 may be a function of the ability of those additives to act as transport media for $IrCl_3$. They would thus prevent the buildup of surface chloride layers in a manner similar to that described by Schäfer and Trenkel (*10*) for the function of AlX_3 in the chlorination reaction of noble metals. Both effects are apparent in the present study. At very low concentrations of CO or NO, active chlorine atoms from the decomposition of $COCl_2$ and NOCl seem to be responsible for the increased reaction rate as products are still deposited in layers around metal particles, but when their concentrations are increased, transport phenomena become more important. Reaction mixtures containing Cl_2 and CO ($4 \geq Cl_2/CO > 2.5$) produced large crystals of α-$IrCl_3$ and $Ir(CO)_3Cl$ on SiO_2. On Al_2O_3 no product phase could be detected with TEM or XRD after treatment in Cl_2 + CO in N_2 ($Cl_2/CO = 4$); only some residual metal particles were apparent after $t_r = 3$ hr. However, the observation that small metal particles were distributed evenly over the alumina after subsequent TPR (Fig. 11e) indicated the presence of a highly dispersed product. In NO + Cl_2 ($Cl_2/NO > 2$), large sheets of α-$IrCl_3$ were observed on SiO_2, but on γ-Al_2O_3, layers of chloride around iridium particles and thin sheets of iridium chloride in the vicinity of partially reacted iridium particles were seen with TEM (Figs. 8a and b), and the presence of small iridium particles after subsequent TPR indicated that on alumina a highly dispersed phase was also formed. This highly dispersed phase was the predominant product after longer reaction times (e.g., $t_r = 3$ hr). In Cl_2 + CO in N_2 with $Cl_2/CO < 2$, the sole product appears as large tubelike crystals (Fig. 7c) or bundles of thick needles (Fig. 7b) which we believe to be $Ir(CO)_3Cl$, and the significant metal losses which are apparent after prolonged treatment are in agreement with the reported high volatility of this compound. In a reaction mixture containing NO and Cl_2 in ratios less than 1, large, thick separate sheets of α-$IrCl_3$, not envelopes, are the main products of the reaction even at lower temperatures (Fig. 8c).

(iii) With Cl_2 + O_2, Cl_2 + O_2 + H_2O, and HCl + O_2 in He. When the reaction gas contains both oxygen and Cl_2, and T_r exceeds 720 K, the products are iridium oxychlorides and iridium oxides. If water is also present, only $IrCl_3$ is formed, even at $T_r = 830$ K. We attribute this to the formation of HCl in the treatment gas. This view is confirmed by the finding that the reaction of catalyst 1 with 10% HCl + 1% O_2 in He at $T_r = 770$ K, $t_r = 2.0$ hr, produced only $IrCl_3$ (Fig. 6). The morphologies and distributions of crystalline products are a result of enhanced chemical transport in those reaction mixtures compared to Cl_2 alone.

Redisperion of the Chloride Phase

In a previous study on the reaction of supported platinum catalysts with chlorine (*4*), we established criteria necessary for effective redispersion of the metal halide phase. These included (i) formation of a volatile metal halide, (ii) redistribution of the halide on the support surface, and (iii) readsorption of the halide and formation of stable surface complexes. In contrast to $PtCl_2$, which is extremely volatile and thus redistributes on the substrate at temperatures as low as 320 K, $IrCl_3$ is significantly less mobile and no substantial transport occurs below 750 K. This is demonstrated by the buildup of significant chloride layers around metal particles and by the fact that the spatial distribution of metal particles in catalyst 2 remains identical before and after chlorination treatment and subsequent reduction (cf. Figs. 4a and c).

The presence of O_2, H_2O, CO, or NO in the reaction mixture caused enhanced chemical transport of Ir with chlorine, but under most conditions the reaction products do not interact strongly enough with

either SiO_2 or Al_2O_3 and large sheets of $IrCl_3$, or $Ir(CO)_3Cl$ are formed. Recently Fung *et al.* and Landolt *et al.* (*13*) have reported a redispersion procedure for iridium-containing catalysts which consisted of the sequence: (i) coke burn off; (ii) reduction; (iii) pretreatment with hydrogen halides in the absence of oxygen in the temperature range 570–820 K; (iv) redispersion in Cl_2, Cl_2–O_2, Cl_2–H_2O, and HCl–O_2 at temperatures above 770 K; and (v) reduction. Of this cycle the pretreatment with hydrogen halides is claimed to be the critical step, and redispersion can be achieved only if the treatment is carried out in the absence of oxygen and the halide level in the catalyst is above a critical value. We have previously identified the criteria for successful redispersion of metals (*4*): (i) formation of volatile compound, (ii) redistribution of the formed compound on the support surface, and (iii) anchoring of the compound on the support surface to prevent agglomeration to large crystals. Considering these criteria, we attribute the claimed success of the treatment described by Fung *et al.* and Landolt *et al.* (*13*) first, to their high redispersion temperature (>770 K) which would enable vapor transport of the formed iridium chloride and second, to a strong interaction of the formed chloride with the highly chlorinated support surface and formation of surface-bound iridium chloride complexes. Our data show that the interaction of iridium chlorides with less chlorinated support surfaces is only weak resulting in the agglomeration of the halide to large crystals, and that evenly distributed chloride phases which, on reduction give rise to small Ir particles, are present only:

(i) with γ-Al_2O_3 supported catalysts and

(ii) after treatment in streams containing Cl_2 and CO (in ratios 2.5 to 4) or Cl_2 and NO (in ratios >2).

We have previously demonstrated (*4*) the different ability of alumina and silica to stabilize highly dispersed platinum chloride phases. For example, on silica, mainly crystalline Pt chlorides were present, whereas on γ-Al_2O_3, a highly dispersed surface complex of Pt(IV) was exclusively formed. This difference has been attributed to the strong interaction of anionic compounds with the alumina but not the silica surface. In analogy to those results with platinum catalysts, we believe that the highly dispersed products here are anionic iridium carbonylchloride (*11*) or iridium nitrosylchloride (*12*) complexes strongly bound to Al_2O_3.

Reduction of Chlorides

TPR profiles of catalysts where Ir is completely converted to $IrCl_3$ show a single reduction peak around 500 K. Catalysts which contain iridium particles surrounded by chloride layers give rise to TPR peaks at 400–440 K. Furthermore, from catalysts which contain both isolated iridium chloride crystals and metal particles with enveloping chloride layers, two reduction peaks are obtained, one below 450 K and the other around 500 K. The chloride layers enveloping Ir particles are thus reduced at a lower temperature. It was found previously that iridium oxide attached to metal particles reduced at lower temperatures than isolated IrO_2 particles, and the effect was explained with the formation of highly active hydrogen atoms on the metal and spillover onto the oxide (*3*).

All crystalline products transform on reduction into large multicrystalline Ir agglomerates which sometimes preserve the general outline of the originating chloride particles. Very small metal particles evenly spread over the support surface are obtained only after the reduction of the highly dispersed chloride phases found in alumina-supported catalysts.

CONCLUSIONS

Agglomerated iridium particles supported on either γ-Al_2O_3 or on SiO_2 are difficult to disperse by treatment with chlorine-containing gases, mainly because of the low volatility of the resultant $IrCl_3$. Gas-

phase transport can be induced by increasing the reaction temperature to above 750 K or by the introduction of O_2, H_2O, CO, or NO to the gas stream. However, under most conditions the products of the reactions do not interact strongly with the substrate and form large crystals, which reduce to agglomerates comparable in size to the originating Ir particles. Redispersion has been achieved with alumina-supported Ir catalysts by treatment in flowing Cl_2 + CO ($4 > Cl_2/CO > 2.5$) in N_2, or in flowing Cl_2 + NO ($Cl_2/NO > 2$) in N_2. The chloride phases responsible for redispersion are believed to be anionic iridium carbonylchloride or nitrosylchloride complexes, stabilized on the alumina surface.

REFERENCES

1. Sittig, M., "Handbook of Catalyst Manufacture." Noyes Data Corp., Park Ridge, N.J., 1978.
2. McVicker, G. B., U.S. Patent 1,541,287.
3. Foger, K., and Jaeger, H., *J. Catal.* **70,** 53 (1981).
4. Foger, K., and Jaeger, H., *J. Catal.* **92,** 64 (1985).
5. Brodersen, K., *Angew. Chem.* **76,** 690 (1964).
6. Rogers, D. B., Shannon, R. D., Sleight, A. W., and Gillson, J. L., *Inorg. Chem.* **8,** 841 (1969).
7. Reis, A. H., Hagley, V. S., and Peterson, S. W., *J. Amer. Chem. Soc.* **99,** 4148 (1978).
8. Bebel, D., and Degner, P., *Z. Anorg. Allg. Chem.* **339,** 57 (1965).
9. Grube, H. L., *in* "Handbook of Preparative Inorganic Chemistry," 2nd ed. (G. Brauer, Ed.), pp. 1592. Academic Press, New York, 1975.
10. Schäfer, H., and Trenkel, M., *Z. Anorg. Allg. Chem.* **414,** 137 (1975).
11. Cleare, M. J., and Griffith, W. P., *J. Chem. Soc. A,* 2778 (1970).
12. McCleverty, J. A., *Chem. Rev.* **79,** 53 (1979).
13. (a) Landolt, G. R., McHale, W. D., and Schoenagel, H. J., GB 2,091,577A; (b) Fung, S. C., Rice, R. W., Weissman, W., Carter, J. L., and Kmak, W. S., EP 0,093,621 A1; U.S. 4,447,551; U.S. 4,444,895; U.S. 4,444,897; U.S. 4,444,896.